Liu *et al.*
Chinese Journal of Mechanical Engineering (2022) 35:36
https://doi.org/10.1186/s10033-022-00696-2

Chinese Journal of Mechanical Engineering

ORIGINAL ARTICLE Open Access

Rail Roughness Acceptance Criterion Based on Metro Interior Noise

Xiaolong Liu[1], Jian Han[2*], Moukai Liu[1], Jianuo Wang[2], Xinbiao Xiao[1] and Zefeng Wen[1]

Abstract

Severe rail roughness leads to a series of problems in metro systems, particularly the vehicle noise problem. To ensure a better acoustic environment, rail roughness control is therefore one of the main concerns for the metro operators. But the existing roughness acceptance criteria are not suitable for metro interior noise control. It is an appropriate method to determine the rail roughness limit based on interior noise. A rail roughness acceptance criterion based on metro interior noise is accordingly proposed in this paper. The relationship between rail roughness and interior noise can be derived with wheel-rail noise as link. With this objective, a combined test and simulation method is adopted. A validated wheel-rfigil noise prediction model is thus established to determine the relationship between rail roughness and wheel-rail noise. Moreover, the transfer function of wheel-rail noise to interior noise is developed based on extensive field test. Using this method, the noise sensitivity to roughness wavelength and acceptance criteria at different speeds and track structures are investigated. Finally, an eclectic rail corrugation acceptance criterion on curved track is suggested in consideration of practical application.

Keywords: Rail roughness, Acceptance criteria, Wheel-rail noise, Interior noise

1 Introduction

In metro systems, typical problems, such as severe noise [1, 2], fastener system failure [3], and bogie damage [4], are mainly caused by the roughness on the rail top surface [5–9]. Firstly, metro lines carry a heavy burden. Simply put, operation density and load are extremely high, particularly during rush hours. Secondly, there are more sharp curves in metro lines where rail corrugation grows at extremely high rates [10, 11], leading to a more intense wheel-rail interaction. In order to provide good riding comfort and travel safety, track maintenance, i.e., rail grinding, is therefore one of the main concerns of metro operators. The maintenance strategy mainly depends on the rail surface condition, which is determined by regular inspection. Current maintenance standards, however, vary with different metro operators.

To ensure a normalised maintenance process, a scientific and practical roughness acceptance criterion is required. Recently, researchers have focused on defining the rail surface roughness limits according to different concerns. Most of them focus on either operation safety or wheel-rail rolling fatigue caused by roughness [12, 13]. For acceptance purposes, the European standard EN 13231-3: 2012 [14] defined two classes of longitudinal profile tolerance, limits are set on the magnitude of the irregularities that can remain in track after a reprofiling operation. Also, it clearly pointed out that this European standard does not apply for acoustic rail reprofiling. In order to improve the wheel-rail contact state and extend the service life of rails, the responsible department of CHINA RAILWAY has formulated a series of rail maintenance operation instructions wherein the rail roughness limits under different situations have been precisely stipulated. The passing by noise control is another major concern. An existing well-known reference for relating roughness with noise is ISO 3095 [15], which defines rail

*Correspondence: hanjian@swjtu.edu.cn
[2] School of Mechanical Engineering, Southwest Jiaotong University, Chengdu 610031, China
Full list of author information is available at the end of the article

corrugation limits based on the passing by noise of a rolling stock.

To alleviate traffic pressure in cities, a large proportion of metro lines are laid underground, where metro trains are confronted with an extreme acoustic environment because of tunnel reverberation [16]. The interior noise of metro trains, to which people are more sensitive than any other indicators, is an important parameter in the evaluation of global comfort as perceived by passengers and train crew, particularly for drivers who are exposed to cacophonous environments over prolonged periods during working hours. It is therefore reasonable to develop a rail grinding strategy based on metro interior noise. The above-mentioned ISO 3095 standard defines the rail corrugation limits based on the passing by noise of rolling stock, but for metro system, interior noise is the main control objective. A scientific and economical strategy based on metro interior noise control is therefore necessary. In order to define the metro-suited roughness acceptance criterion, the relationship between rail roughness and interior noise is established in this study, and the metro interior noise limit is considered as the control objective. The remainder of this paper is organised as follows: first, an experimental study of the effect of rail roughness on the interior noise is presented in Section 2.1. Thereafter, the roughness acceptance criterion estimation method, wheel-rail noise prediction model, and their validation are introduced in Section 2.2. Then, the related results under various operation conditions are presented in Section 3.2 and 3.3. Finally, an eclectic rail corrugation acceptance criterion on curved track in consideration of practical application is suggested in Section 3.4.

2 Methodology

The wheel-rail noise mechanism has been widely known over the past few decades, particularly after the introduction of TWINS, which is a prominent prediction model [17, 18]. Metros in China typically operate at 40–80 km/h, with some lines running at up to 120 km/h. At these speeds the dominant source of noise from the railway is rolling noise, which is excited by rail roughness.

2.1 Experimental Study: Effect of Rail Roughness on Interior Noise

To resolve the noise problem of metro lines in the major cities of China, in recent years, a group tasked by the authors has been conducting field tests in which the wheel/rail roughness and sound emission of the train are measured. Figure 1 shows the roughness measurement process. Rail roughness is measured using corrugation analysis trolley (CAT), the position of the sensor should be adjusted according to the rail condition in order to accurately measure the roughness on the contact surface. The noises at the wheel-rail area and inside the carriage are measured simultaneously, as shown in Figure 2.

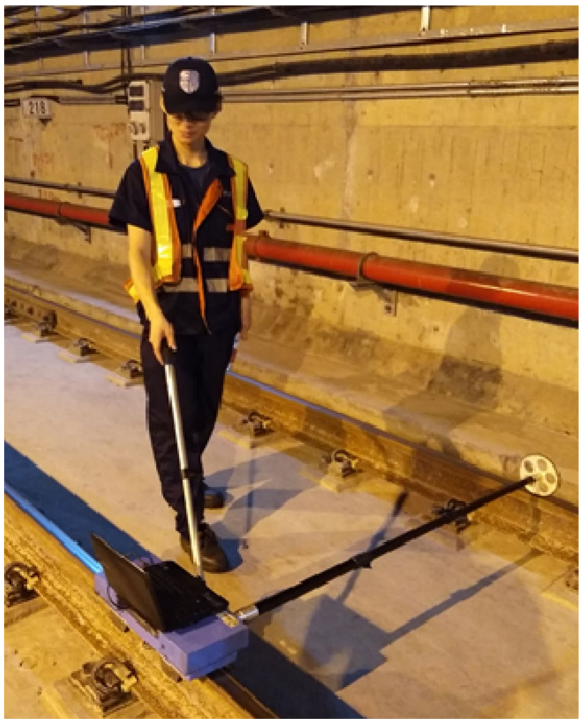

Figure 1 Roughness measurement

Numerous characteristics of noise and roughness are obtained through field tests. It should be noted that several measured metro lines experience severe noise problems, typical examples are shown in Figure 3. The upper diagram in Figure 3 shows that the interior noises in more than 88% of the operation sections in one line exceed the limit. The lower diagram in Figure 3 provides a time history of the interior noise when the vehicle runs in a section. It is found that the instantaneous sound pressure exceeds 100 dBA. Those variation is attributed to different degrees of rail roughness along the track.

Figures 4 shows the effect of rail roughness on the interior noise. Generally speaking, the corresponding wavelength of the significantly high roughness level varies with the track structure type, this is usually called rail corrugation, as shown in Figures 4(a). Before rail grinding, there is a severe rail corrugation in the 25–63 mm wavelength range. After rail grinding, the amplitude of rail corrugation in this wavelength range significantly decreases. When the operational speed is approximately 60 km/h, the interior noise spectrum difference caused by rail corrugation is reflected in the 297–591 Hz frequency range (Figures 4(b)) according to the relationship

Figure 2 Wheel-rail noise and interior noise measurement

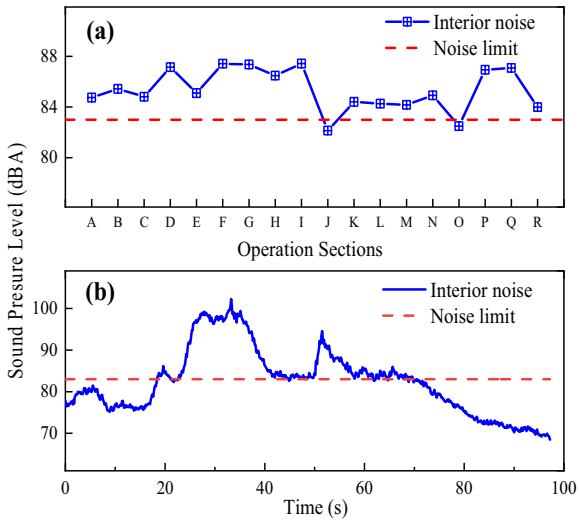

Figure 3 Characteristics of severe noise

between running speed, wavelength, and excitation frequency given by the following equation:

$$f = \frac{v/3.6}{\lambda/1000}, \tag{1}$$

where f is the excitation frequency; v is the running speed (km/h); λ is the wavelength (mm).

2.2 Research Methodology, Prediction Model, and Validation

The analysis in Section 2.1 reveals a strong relationship between interior noise and rail roughness. It is therefore feasible to define a rail roughness acceptance criterion

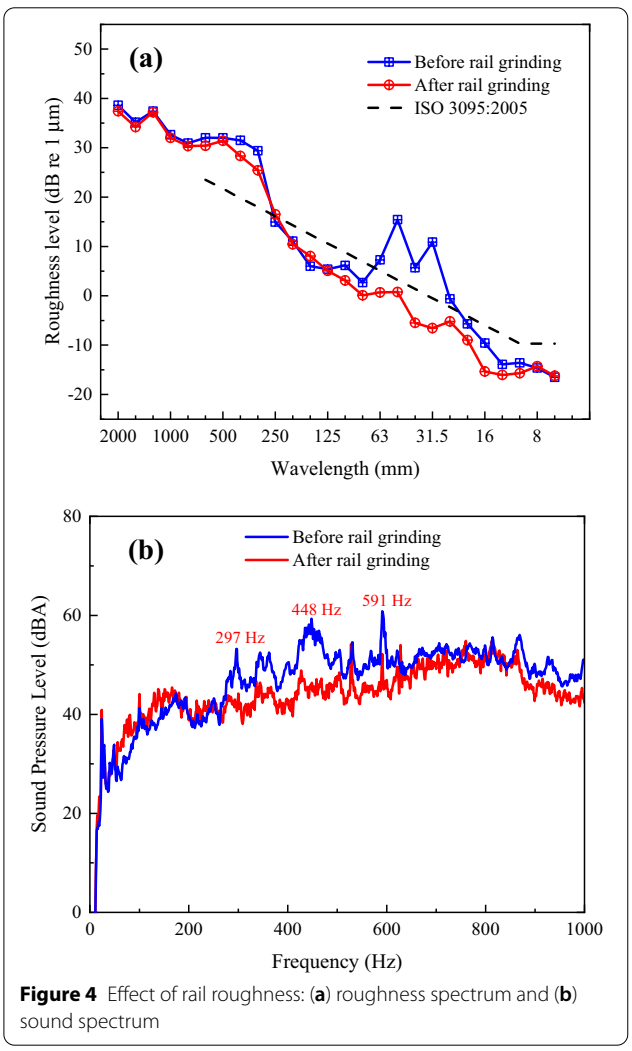

Figure 4 Effect of rail roughness: (**a**) roughness spectrum and (**b**) sound spectrum

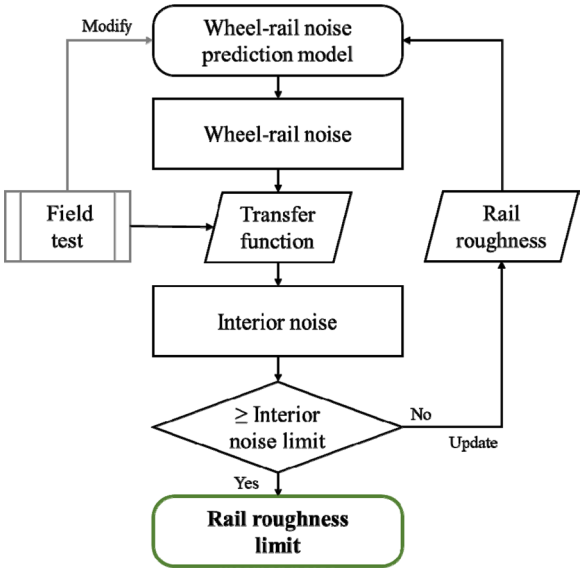

Figure 5 Determination method of roughness acceptance criteria

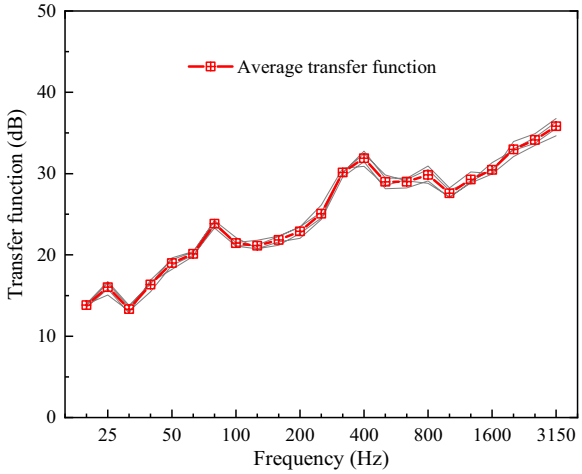

Figure 6 Transfer function

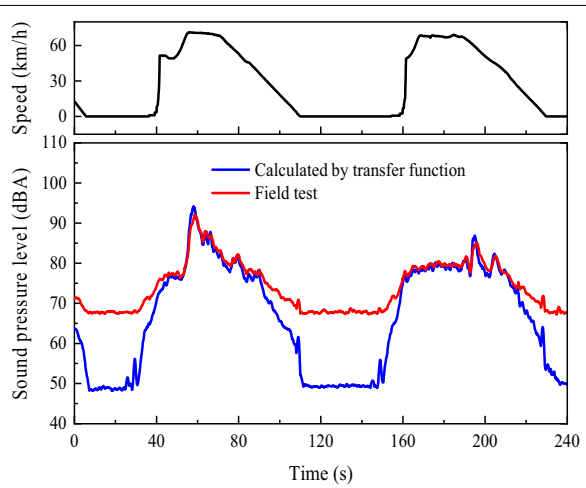

Figure 7 Validation of interior noise evaluation method

Table 1 Metro vehicle interior noise limits [19]

Location	Operation environment	Noise limits (dBA)
Driver's cab	Ground	75
	Underground	80
Carriage	Ground	75
	Underground	83

based on the interior noise. A combined test and simulation method is used in this research to determine the rail maintenance strategy, as shown in Figure 5. First, throughout the research process, different levels of rail roughness are employed as input excitation, and the wheel-rail noise acts as a part of the link between the interior noise and rail roughness. A wheel-rail noise prediction model is accordingly established and modified by test results. The wheel-rail noise could be affected by several factors, such as running speed and infrastructure, which will be discussed in the following section. Second, the car body sound transfer function concept, which is another important indicator that influences interior noise, is employed. An average transfer function is therefore calculated based on test data. Finally, considering the interior noise limit value as a boundary condition, the interior noise is obtained to determine the critical roughness values under different conditions. The metro interior noise limit value may vary from country to country, in this study the Chinese metro interior noise limit [19] is adopted, as summarised in Table 1.

The transfer function of the train is obtained by calculating the difference value between wheel-rail noise and interior noise in frequency domain. Figure 6 shows the sound transfer function of a B-type metro vehicle, which runs in the tunnel. In Figure 6, the grey solid lines and red dotted line indicate the measured data in several operation sections and the average transfer function, respectively. The feature of the function is relatively stable. To verify the reliability of the transfer function and illustrate its scope of application, a comparison between the calculated and measured interior noises in the two consecutive sections is shown in

Figure 7. The black solid line in the upper graph is the train speed. The lower graph shows that the calculated and measured results are in good agreement when the train speed is increased to a certain level. On the contrary, when the speed is lower or the train is motionless, there is a considerable difference between the two results. This is because wheel-rail noise is insignificant when the speed is low, and the interior noise is mainly affected by the auxiliary equipment, e.g., air conditioning and car radio. As a result, the measured values are considerably higher than those calculated based only on wheel-rail noise. It can be concluded that the interior noise calculation method is reliable when the wheel-rail noise is the dominant sound source. With this premise, an accurate wheel-rail noise prediction model is the most important aspect that should be established.

The wheel-rail interaction deforms the contact area. The roughness with wavelength shorter than the size of the wheel-rail contact area does not have any excitation effect on the wheel-rail system, this is called contact filter. A filter function, adopted from Ref. [20], is expressed by

$$\left|H(k)\right|^2 = \frac{4}{\alpha(kb)^2}\int_0^{\arctan\alpha}[J_1(kb\sec x)]^2\mathrm{d}x, \tag{2}$$

where k is the wavenumber of the roughness; b denotes the equivalent radius of the contact zone; J_1 is the 1st Bessel function; α denotes the correlation coefficient of roughness on the interaction surface.

The roughness after contact filtering is an effective combined roughness, which is the real excitation source [20]:

$$L_{r\_total} = 10\lg\left(10^{L_{r\_wheel}/10} + 10^{L_{r\_rail}/10}\right) + 10\lg\left|H(k)\right|^2, \tag{3}$$

where L_{r_wheel} and L_{r_rail} denote the wheel and rail roughness (dB), respectively.

The contact force on the wheel-rail interaction surface is expressed as Eq. (4) [20].

$$F_c = -\frac{r}{\alpha_{\mathrm{W}} + \alpha_{\mathrm{R}} + \alpha_{\mathrm{C}}}, \tag{4}$$

where r denotes the combined roughness (m); α_{W} and α_{R} are the vertical receptance of wheel and rail, respectively; α_{C} denotes the contact receptance of the wheel-rail contact area. Detailed information can be found in Ref. [7]. The wheel-rail contact force acts as an input excitation to calculate the wheel-rail response. Finally, the wheel-rail noise is calculated with the boundary integral equation [21]:

$$\overline{p}(x,y,z) = -\int_S (\overline{p}(x',y',z')\frac{\partial G(R)}{\partial n} + i\rho\omega G(R)v_n(x',y',z'))\mathrm{d}S, \tag{5}$$

where $\overline{p}(x,y,z)$ denotes the amplitude of the sound pressure; v_n (x', y', z') is the normal velocity of the vibration surface; $G(R)$ is Green function. The equation is solved by the three-dimensional (3D) boundary element method.

In order to translate the wheel-rail interaction into noise radiation, the natural characteristics of wheel/rail, i.e., receptance, and contact receptance must be obtained first. An ordinary metro wheel and common slab track vibration prediction model is firstly established based on the finite element method (FEM), as shown in Figure 8(a). The wheel, rail, and slab are discretised by solid elements, and the fastener system is simulated by spring-damper elements. To verify the reliability of the model, hammer tests are performed to measure the dynamic characteristics of the slab track and wheel, as shown in Figure 8(b) and (c), respectively. In the wheel test, an ordinary metro wheel is hung freely by an elastic rope to simulate a free-free boundary condition. Meanwhile, the accelerometers are mounted at the tread, rim, and web. The wheel is thereafter excited with a force sensor-mounted hammer. The track test is conducted on a metro line with the sensors mounted on the rail head, and a hammer with a force sensor is employed to excite the rail. Figure 8(d) and (e) show the comparison results between the simulated and measured receptance. It is found that the results well match in most of the inherent frequencies, indicating that the prediction model could be regarded as reliable for reflecting the wheel-rail dynamic feature.

3 Roughness Acceptance Criteria

The necessity and feasibility of defining the roughness acceptance criterion based on interior noise have been discussed in the first two sections. In this section, detailed roughness acceptance criteria under different operational conditions are discussed, so that we can have an insight into the influencing factors on roughness limit. Also, in consideration of practical application, an eclectic rail corrugation acceptance criterion is suggested. It is anticipated that the corresponding results may provide a reference for metro rail maintenance.

The effective combined roughness is the real excitation source for the wheel-rail system. This means that when the wheel-rail noise or combined roughness is fixed, the wheel and rail roughness are a couple of inter-limitation parameters, as shown in Figure 9. If the rail

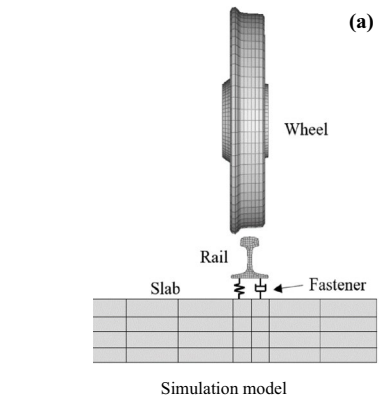

Simulation model

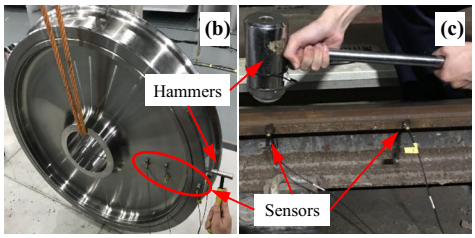

Wheel dynamic character test Rail dynamic character test

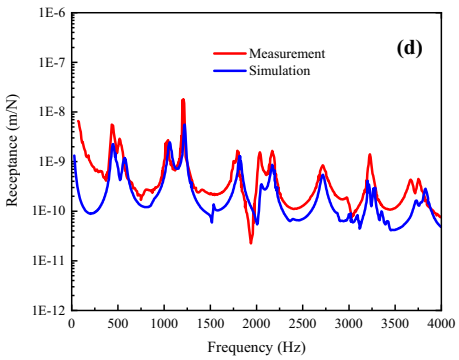

Wheel validation

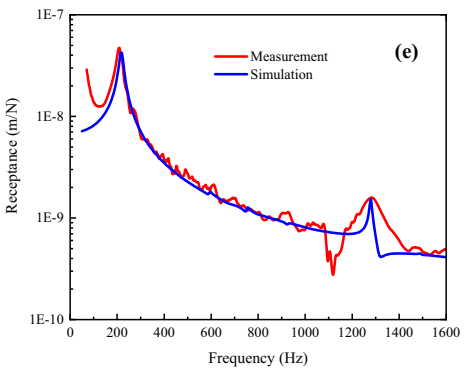

Rail validation

Figure 8 Wheel-rail noise prediction model and validation

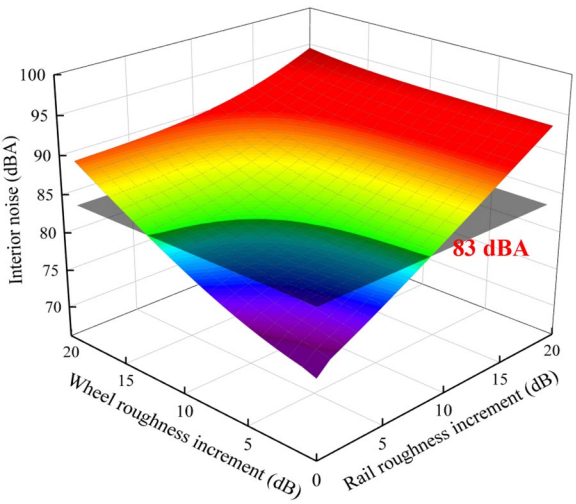

Figure 9 Relationship between wheel/rail roughness and interior noise

roughness acceptance criterion is defined based on a rough wheel, then the rail roughness limit will be strict. On the contrary, it will be extremely relaxed when the wheel is smooth. Considering that the wheel roughness spectra measured in many metro lines are similar to the A-class wheel roughness spectrum in Ref. [22], so, when rail roughness acceptance criteria is discussed, the wheel roughness is fixed in A-class spectrum to eliminate its influence. As a reference for rail roughness, ISO 3095 is widely used and it is at a modest level. The reference roughness spectrum is shown in Figure 10.

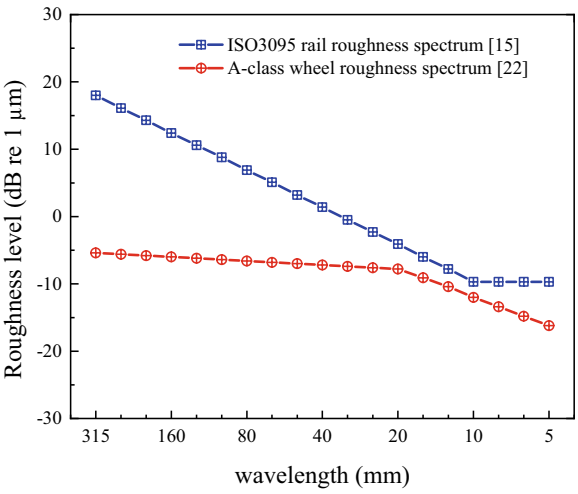

Figure 10 Reference standard of wheel/rail roughness

3.1 Noise Sensitivity to Roughness Wavelength

The complexity of rail corrugation is mainly indicated by the following. (1) A wide range of wavelength. Rail corrugation can be classified into three types according to wavelength [23]: short-pitch rail corrugation (20–75 mm), long wavelength corrugation (75–600 mm), and extremely long wavelength ($\geq$ 600 mm). (2) The feature of rail corrugation varies with the type of track structure and curve radius. After measuring several metro lines, it was found that the most common wavelengths of rail corrugations are 31.5–50 mm [13].

Whether the roughness in the all-wavelength range have the same effect on the interior noise or not is yet to be determined. The noise sensitivity to roughness wavelength is investigated herein. Figure 11 presents the relationship between interior noise and roughness wavelength at a speed of 60–120 km/h. As shown in the figure, not all roughness has the same contribution to interior noise. When the operation speed is 60 km/h, the sensitive wavelength is in the range of 10–63 mm, particularly in 16–31.5 mm. As the speed increases, the sensitive wavelength band shows minimal movement toward the longer wavelength. The dominant frequency range of the wheel-rail noise is responsible for the local high sensitivity. In the meantime, the roughness, whose contribution is not in the dominant frequency range, has a minimal effect on the interior noise. Additionally, the movement of the sensitive band can be explained by the relationship between excitation frequency, wavelength, and train speed, as shown by Eq. (1). With the increase in speed, a roughness with a longer wavelength is necessary to provide the same excitation frequency.

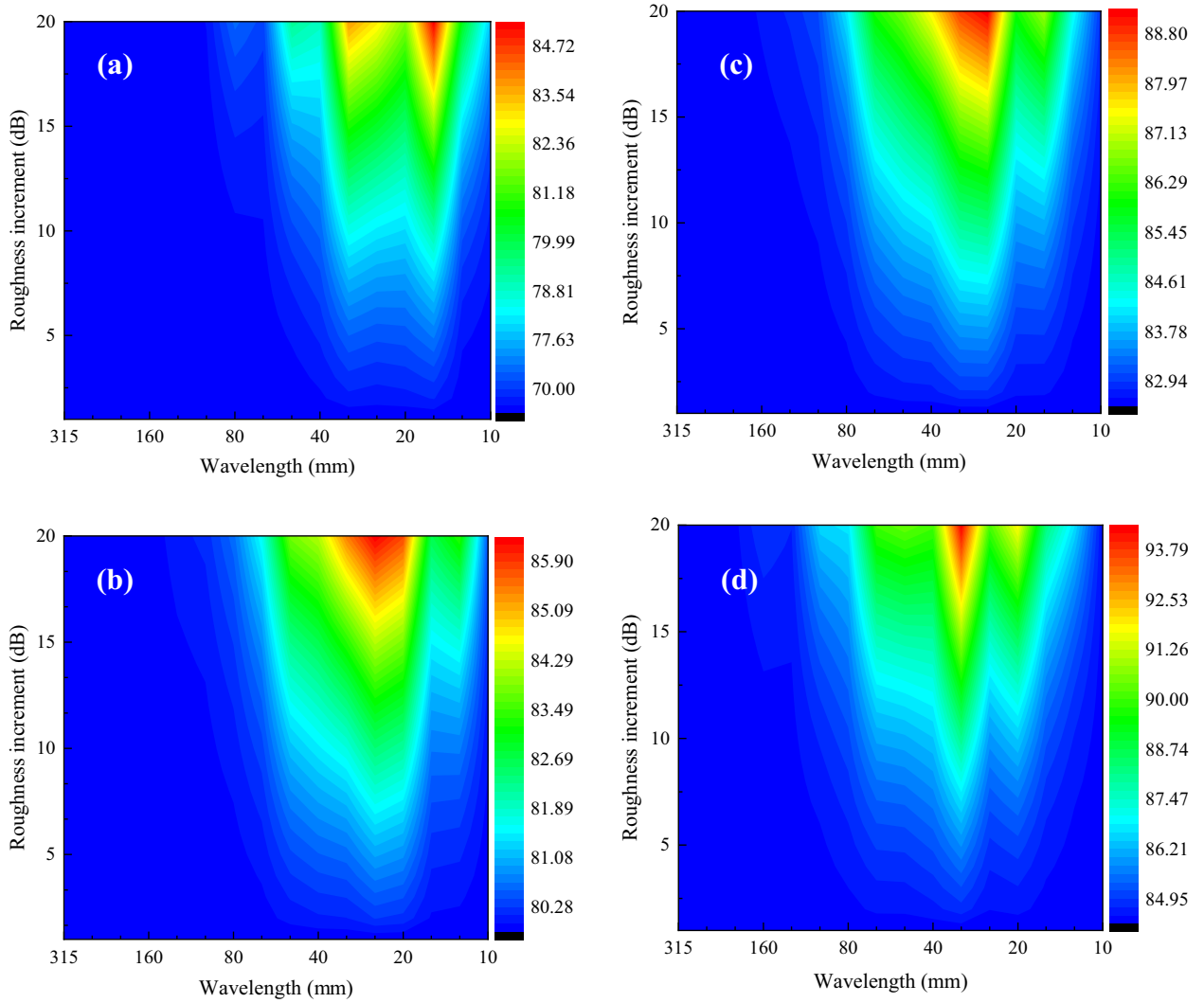

Figure 11 Wavelength sensitivity analysis: (**a**) $v = 60$ km/h; (**b**) $v = 80$ km/h; (**c**) $v = 100$ km/h; (**d**) $v = 120$ km/h

So, the interior noise is most sensitive to the roughness with wavelength in 20–63 mm band. Furthermore, this wavelength band has contained the most common corrugation wavelength band in field track. In the following investigation, this "sensitive wavelength band" deserves special attention.

3.2 Acceptance Criteria at Different Operation Speeds

The operation speed of the metro system in China is in the range 40–80 km/h (some lines run at 120 km/h). With the increase in speed, the interaction force between wheel and rail become more intense, as well as the sound radiation. This means that the roughness acceptance criteria will vary with speed since the noise limit is fixed.

Figure 12(a) shows the predicted effect of rail roughness on interior noise for a train at 60 km/h and the following three cases of rail roughness are considered: 5–315 mm ("all" wavelengths), 20–63 mm (sensitive wavelength band) and 31.5–50 mm (common wavelength band). If rail roughness were at the ISO 3095 limit, the interior noise level would be 76 dBA. If the roughness were increased uniformly by 7 dB over "all" wavelengths (5–315 mm), the interior noise level would reach the proposed 83 dBA limit (Table 1). If roughness were increased over the "sensitive" wavelength range only (20–63 mm), an increase of 8 dB would be possible before exceeding the 83 dBA limit on interior noise whereas an increase in roughness of 12 dB would be necessary over only the "common" wavelength band (31.5–50 mm). Figure 12(b) shows the spectra of interior noise and responses of interior noise in different frequency bands to the three cases of rail corrugation.

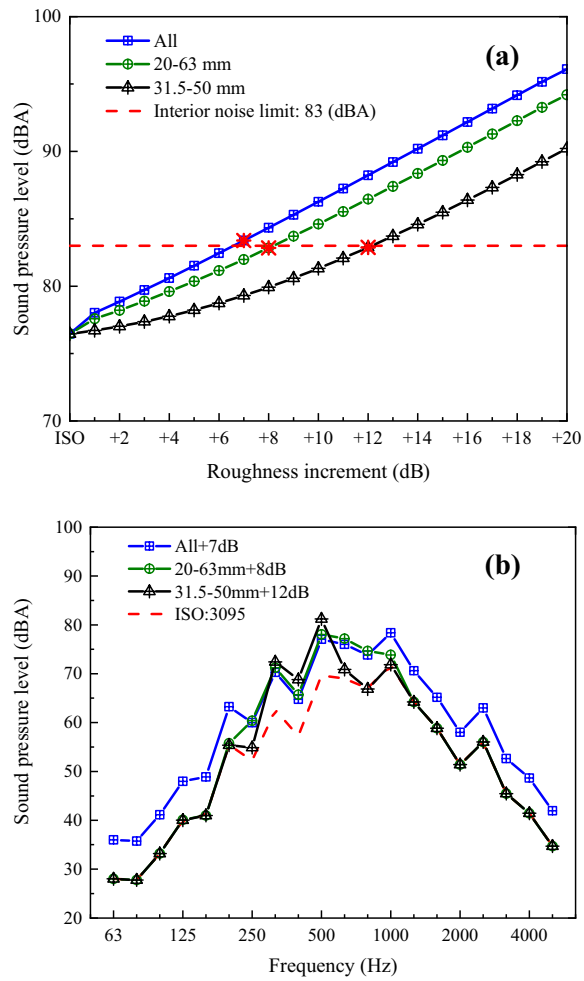

Figure 12 Effect of rail corrugation on interior noise: (**a**) overall and (**b**) frequency spectrum

Figure 13 illustrates the acceptance criteria of three types of rail roughness at a speed of 60 km/h. The acceptance criteria are described as follows, when the rail is corrugated in a large wavelength band, the roughness level should not exceed the blue dotted line. If the remarkable corrugation only exists in the sensitive band (20–63 mm), then the roughness level should not exceed the green dotted line. If the remarkable corrugation only exists in the common band (31.5–50 mm), the roughness level should not exceed the black dotted line.

Figure 14 illustrates the rail roughness acceptance criteria for the all-wavelength band in the 40–120 km/h speed range. With an increase in speed, the rail roughness level should be continuously reduced. When the operation speed is less than 100 km/h, the rail roughness acceptance criteria are relatively less stringent than the ISO 3095 limit. If ISO 3095 continues to be used to evaluate the rail roughness, then this will lead to excessive maintenance and increase in maintenance cost. On the contrary, when the speed is higher than

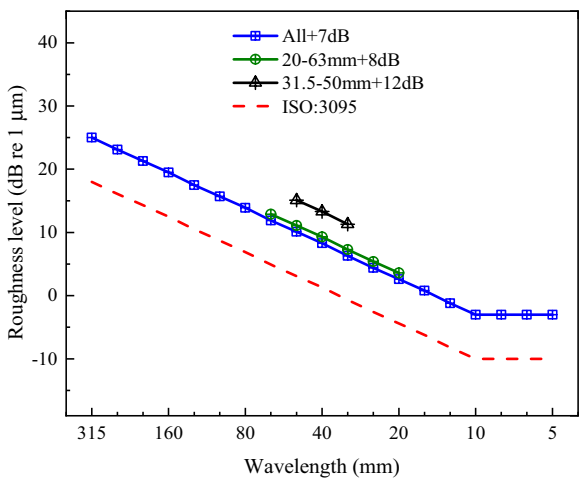

Figure 13 Rail roughness acceptance criteria at 60 km/h

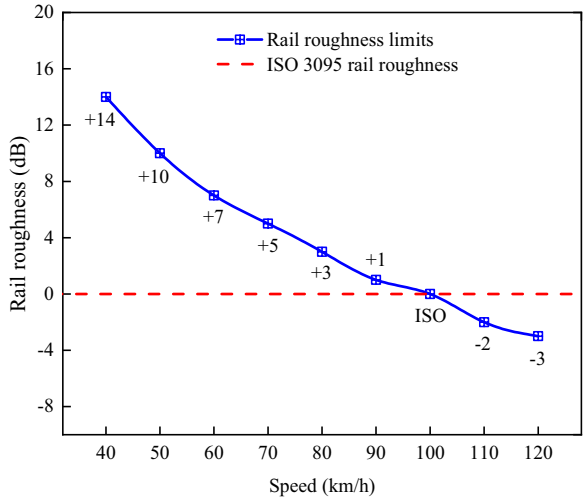

Figure 14 Rail roughness acceptance criteria for all-wavelength band at different speeds

Table 2 Rail roughness limits at different speeds

Speed (km/h)	Rail roughness limit (dB)		
	All-wavelength band: 5–315 mm	Sensitive band: 20–63 mm	Common band: 31.5–50 mm
40	ISO+14 dB	ISO+16 dB	/
50	ISO+10 dB	ISO+12 dB	ISO+19 dB
60	ISO+7 dB	ISO+8 dB	ISO+12 dB
70	ISO+5 dB	ISO+6 dB	ISO+10 dB
80	ISO+3 dB	ISO+3 dB	ISO+7 dB
90	ISO+1 dB	ISO+1 dB	ISO+4 dB
100	ISO	ISO	ISO
110	ISO−2 dB	ISO−2 dB	ISO−3 dB
120	ISO−3 dB	ISO−3 dB	ISO− dB

100 km/h, the rail roughness acceptance criteria are relatively stricter than the ISO 3095 limit. Hence, when ISO 3095 is used to measure the rail roughness, it will lead to insufficient maintenance and severe noise emissions. Three types of detailed rail roughness acceptance criteria at different speeds are summarised in Table 2.

3.3 Acceptance Criteria at Different Track Structures

Several types of vibration isolation tracks, such as rubber-booted short sleeper track, floating slab, and ballast track, are employed in metro lines to satisfy the vibration isolation requirement. In order to establish a systematised roughness acceptance criterion, different types of track structures must be considered. The rubber-booted short sleeper track and ballast track are taken as examples in the present work. The simulation models for the two foregoing tracks are established based on the FEM, as shown in Figure 15. In the models, the fastener, the rubber pad under the sleeper of the rubber-booted short sleeper track, and the ballast of the ballast track are simulated by spring-damping elements. In order to validate the accuracy of the prediction model, Figure 16 shows a comparison between the calculated and measured receptance values; it is found that the results agree well. It should be noted that because there is no measurement result for the ballast track, the FEM result is validated by the TWINS model.

The interior noises under these three types of tracks are shown in Figure 17. It is found that the difference in the value of the overall interior noise between the slab track and rubber-booted short sleeper track is only 0.7 dBA under the same rail roughness excitation. In the significant noise frequency band of 500—1000 Hz, there is practically no difference between the two. That is, the roughness acceptance criteria under these two types of tracks can be considered the same from the perspective of interior noise control. The overall value of the ballast track, however, is 3.2 dBA lower than that of the slab track. A remarkable difference appears in most frequency ranges, especially in the significant noise frequency band. Simply put, the roughness acceptance criterion for the ballast track is relatively different from that of the slab track.

Figure 18 shows the acceptance criteria for the three types of rail roughness for the ballast track at a speed of 60 km/h. The interior noise exhibits a higher tolerability to roughness because of the lower sound radiation of the ballast track, indicating that its roughness acceptance criterion can be appropriately relaxed without generating excessive interior noise.

In reality, the sound radiations of many vibration isolation tracks as well as the common slab track with damping fasteners slightly differ from those of the slab track with a common fastener. The roughness acceptance criteria based on interior noise can be considered the same, and no further detailed description is provided here. The type of wheel is another factor which might affect the wheel-rail noise and further affects the rail roughness limits. In fact, compared to common rigid wheel, most low-noise wheels can effectively reduce the sound radiation of the wheels themselves. However, since the wheel-rail noise is dominated by the sound radiation of track, only reducing the sound radiation of wheel has little effect on the total wheel-rail noise [6]. However, the resilient wheel is an exception. Because the web and rim are decoupled by the rubber blocks, which leads to a decrease on the unsprung mass [24]. In this situation, the wheel-rail force under the same roughness will be decrease, which leads to a smaller track noise radiation,

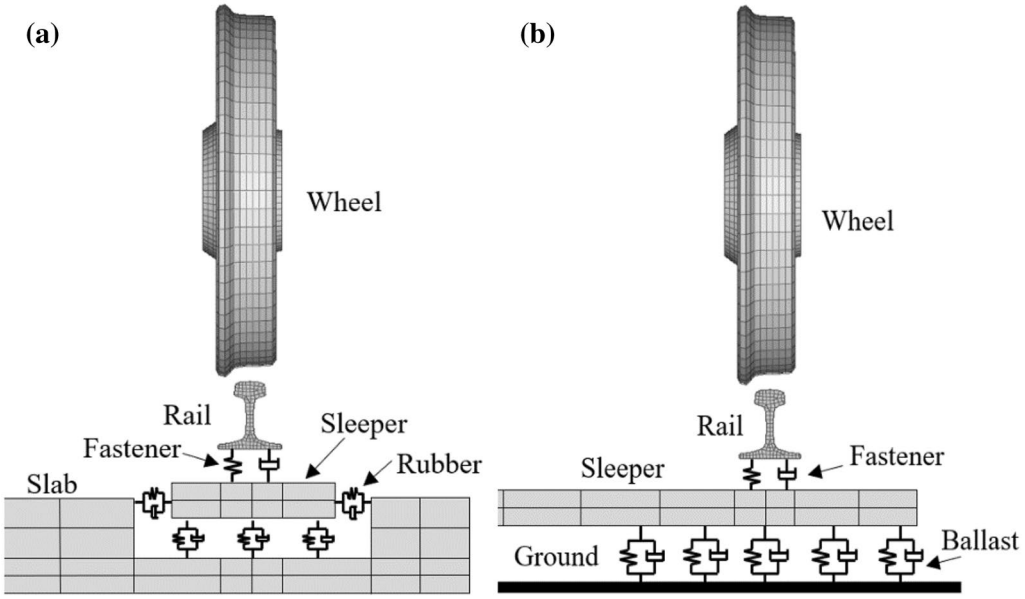

Figure 15 Simulation model: (**a**) Rubber-booted short sleeper track and (**b**) Ballast track

as well as the total wheel-rail noise. As a result, the rail roughness limit under resilient wheel will be different with that of the common rigid wheel. However, considering that the resilient wheels are currently mainly used in trams, and resilient wheels for metros are still in the research and test stage, therefore, the influence of the wheel on the rail roughness limit is not considered in this work.

3.4 Acceptance Criteria for Practical Application

In Sections 3.2 and 3.3, the rail roughness acceptance criteria at different operation conditions have been discussed in detail. With those conclusions, we have a better understanding in the influence factors on rail roughness acceptance criteria. Theoretically, it would be more reasonable to define the rail roughness acceptance criteria at different operation conditions; however, it appears to be tedious and not applicable for routine maintenance in terms of practical applications. A compromise must therefore be proposed to reach a balance between scientificity and practicability.

Rail corrugations occurring on the curves are the most serious in the railway field [10, 11], one of the reasons is that the lateral motion of the rails at the curved track occurs more easily and is much fiercer than the rails at the tangent track due to the lateral attack of the wheelset. That means the metro interior noise on curved track is much more serious than it on tangent track, this is confirmed by a large amount of field test. So, the curved track is the main site to be maintained.

The traveling speed of metro train on curve usually determined by the necessity of routine operations and the radius of curve. In general, the curve radius of the majority of track are in the range of 300–500 m, and the corresponding operation speed is in the range of 60–80 km/h [13, 25]. Considering both noise control and cost saving, the rail roughness acceptance criteria on curve determined by the result of the speed at 70 km/h is reasonable. The main attention is still focused on the wavelength range of 20–63 mm, as shown in Figure 19, and the roughness with wavelength longer than 63 mm or shorter than 20 mm may not be paid much attention here, because they have little influence on noise emissions. For the longer or shorter roughness, they could be limited by other criteria for a certain purpose. Furthermore, track types are no longer distinguished since the sound radiation character between slab tracks is not remarkable, and the ballast track is less used recently. Even if ballast track is still widely used in some countries, the criterion of slab track is enough to ensure an eligible noise condition of ballast track, because the criterion of ballast track is less demanding than that of slab track, as stated in Section 3.3.

4 Conclusions

A combined test and simulation method is used to investigate the effect of rail roughness on interior noise. Wheel-rail noise prediction models and the relationship between interior noise and rail roughness are established

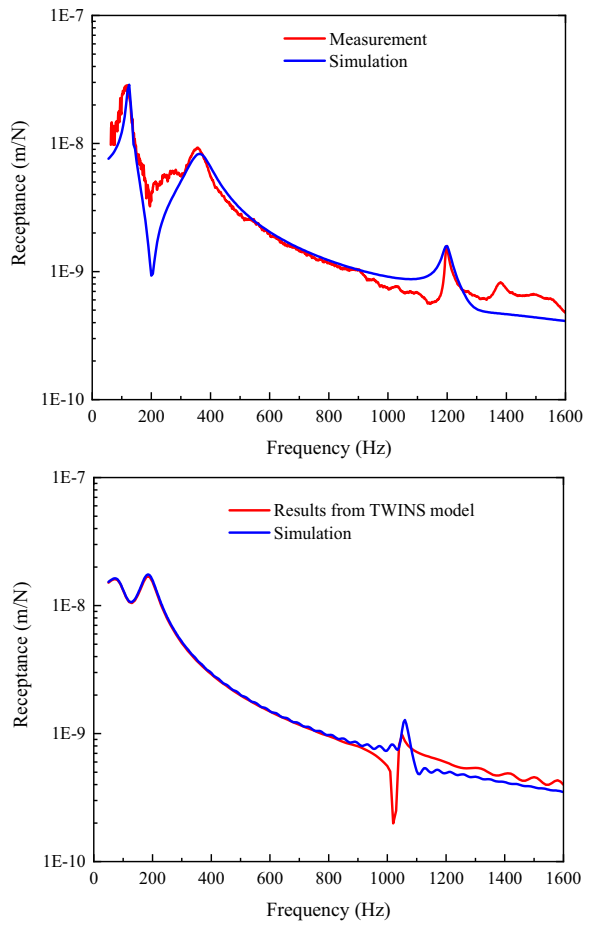

Figure 16 Wheel-rail noise prediction model validation: (**a**) Rubber-booted short sleeper track and (**b**) Ballast track

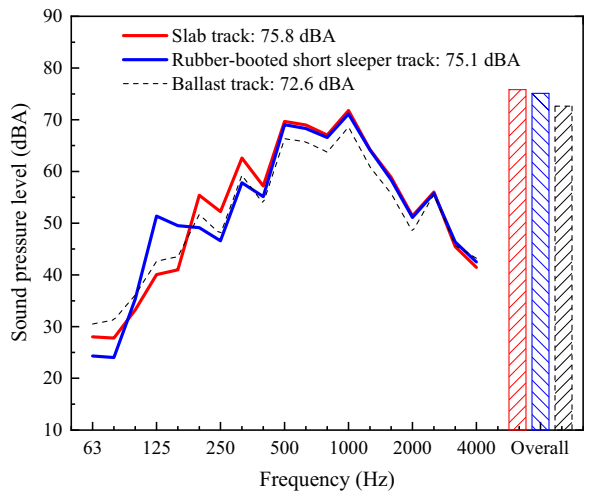

Figure 17 Interior noises under different track structures

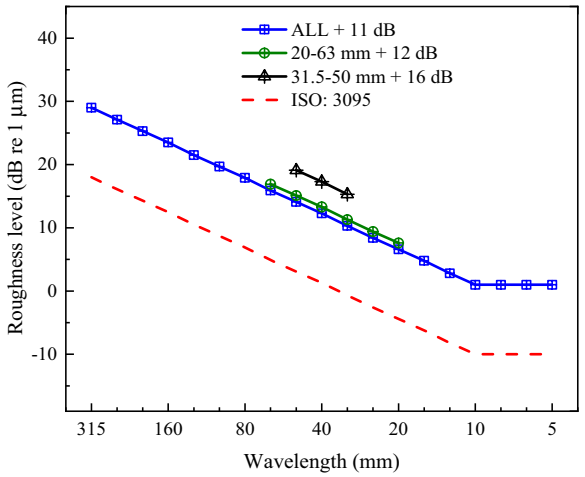

Figure 18 Rail roughness limits for ballast track at 60 km/h

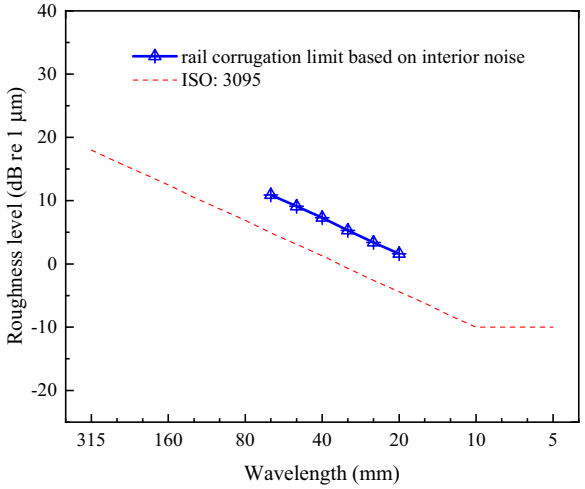

Figure 19 Rail corrugation acceptance criteria on curve

and validated. The interior noise calculation method is reliable when the wheel-rail noise dominates the whole metro noise. Additionally, the dynamic features of wheel-rail noise prediction models match well with measured results.

With the prediction models and calculation method, the sensitivity of noise to the roughness wavelength is investigated. This parameter is related to the running speed and remarkable wheel-rail noise frequency range. For the general metro system, noise radiation has a high sensitivity to short-pitch (20–63 mm) roughness. The interior noise-based roughness acceptance criterion varies with the operation speed and track structure. It is imperative to determine the systematic roughness acceptance criterion so that either

insufficient or excessive maintenance can be avoided to the extent possible. However, practical application has much difference with academic research, so, an eclectic rail corrugation acceptance criterion on curved track have been provided to meet the requirement of practical application.

It should be emphasised that the transfer function may be influenced by the operation environment (tunnel and bridge) and types of vehicles. For a certain metro line, however, the vehicle type is decided, and the operation speed and track types in every section are determined. A modular roughness acceptance criterion analysis method is proposed in this work; hence, variational parameters, such as track structures and transfer functions, in different metro lines can be regarded as input data to obtain the roughness acceptance criterion under different situations.

Acknowledgements
The authors thank Jian Kai, Ting-Sheng Zhong, Zi-Wei Zhu, Peng Wang, and Gong-Quan Tao for their assistance in conducting the experiment and data analysis.

Authors' contributions
XL was in charge of modeling and writing the manuscript; JH, ML and JW assisted with investigation; XX and ZFW were in charge of review and editing. All authors read and approved the final manuscript.

Authors' information
Xiaolong Liu, born in 1990, is currently a PhD candidate at *State Key Laboratory of Traction Power, Southwest Jiaotong University, China*.
Jian Han, born in 1987, is currently a research assistant at *School of Mechanical Engineering, Southwest Jiaotong University, China*. He received his PhD degree from *Southwest Jiaotong University, China*, in 2018. His research interests include the railway vibration and noise reduction.
Moukai Liu, born in 1993, is currently a PhD candidate at *State Key Laboratory of Traction Power, Southwest Jiaotong University, China*.
Jianuo Wang, born in 1996, is currently a PhD candidate at *School of Mechanical Engineering, Southwest Jiaotong University, China*.
Xinbiao Xiao, born in 1978, is currently an associate researcher at *State Key Laboratory of Traction Power, Southwest Jiaotong University, China*. He received his PhD degree from *Southwest Jiaotong University, China*, in 2013. His research interests include the railway vibration and noise reduction.
Zefeng Wen, born in 1976, is currently a researcher at *State Key Laboratory of Traction Power, Southwest Jiaotong University, China*. He received his PhD degree from *Southwest Jiaotong University, China*, in 2006. His research interests include the wheel-rail interaction.

Funding
Supported by the National Nature Science Foundation of China (Grant No. 52002340), the National Natural Science Foundation of China (Grant No. U1834201), and China Postdoctoral Science Foundation (Grant No. 2020M673280).

Competing interests
The authors declare no competing financial interests.

Author Details
[1]State Key Laboratory of Traction Power, Southwest Jiaotong University, Chengdu, China. [2]School of Mechanical Engineering, Southwest Jiaotong University, Chengdu 610031, China.

Received: 12 June 2021 Revised: 29 January 2022 Accepted: 21 February 2022
Published online: 09 April 2022

References

[1] J Han, X B Xiao, Y Wu, et al. Effect of rail corrugation on metro interior noise and its control. *Applied Acoustics*, 2018, 130: 63-70.
[2] J Zhang, G X Han, X B Xiao, et al. Influence of wheel polygonal wear on interior noise of high-speed trains. *Journal of Zhejiang University- Science A*, 2014, 15: 1002-1018.
[3] J H Wei, C Liu, T Q Ren, et al. Online condition monitoring of a rail fastening system on high-speed railways based on wavelet packet analysis. *Sensors*, 2017, 17: 318.
[4] R K Luo, B L Gabbitas, B V Brickle, et al. Fatigue damage evaluation for a railway vehicle bogie using appropriate sampling frequencies. *Vehicle System Dynamics*, 1998, 29: 404-415.
[5] S L Grassie. Rail corrugation: advances in measurement, understanding and treatment. *Wear*, 2005, 258: 1224-1234.
[6] D J Thompson. On the relationship between wheel and rail surface roughness and rolling noise. *Journal of Sound & Vibration*, 1996, 193: 149-160.
[7] D J Thompson. Railway noise and vibration: mechanisms, modelling and means of control. *Elsevier Science & Technology*, 2008, 153: 21-25.
[8] X S Jin, Z F Wen, K Y Wang, et al. Three-dimensional train-track model for study of rail corrugation. *Journal of Sound & Vibration*, 2006, 293: 830-855.
[9] X S Jin, L Wu, J Fang, et al. An investigation into the mechanism of the polygonal wear of metro train wheels and its effect on the dynamic behaviour of a wheel/rail system. *Vehicle System Dynamics*, 2012, 50: 1817-1834.
[10] X S Jin, Z F Wen, W H Zhang, et al. Numerical simulation of rail corrugation on a curved track. *Computers & Structures*, 2005, 83: 2052-2065.
[11] Z F Wen, X S Jin. Effect of track lateral geometry defects on corrugations of curved rails. *Wear*, 2005, 259: 1324-1331.
[12] J C O Nielsen, A Ekberg. Acceptance criterion for rail roughness level spectrum based on assessment of rolling contact fatigue and rolling noise. *Wear*, 2011, 271: 319-327.
[13] W Li. Study on root cause of metro rail corrugation and its influence on behavior of vehicle-track system, *Southwest Jiaotong University*, 2015, (in Chinese).
[14] Netherlands Standardization Institute. EN 13231-3: 2012. Railway applications - track - acceptance of works - part 3: Acceptance of reprofiling rails in track. delft: Netherlands Standardization Institute, 2011.
[15] International Organization for Standardization. ISO 3095: 2005. Acoustics - Railway Applications - Measurement Of Noise Emitted By Railbound Vehicles. Switzerland: International Organization for Standardization, 2004.
[16] S Sanok, F Mendolia, M Wittkowski, et al. Passenger comfort on high-speed trains: effect of tunnel noise on the subjective assessment of pressure variations. *Ergonomics*, 2015, 58: 1022-1031.
[17] D J Thompson, B Hemsworth, N Vincent. Experimental validation of the TWINS prediction program for rolling noise, part 1: Description of the model and method. *Journal of Sound and Vibration*, 1996, 193: 123-135.
[18] D J Thompson, P Fodiman, H Mahé. Experimental validation of the TWINS prediction program for rolling noise, part 2: Results. *Journal of Sound & Vibration*, 1996, 193: 123-35.
[19] General Administration of Quality Supervision, Inspection and Quarantne of People's Republic of China; Standardization Administration of People's Republic of China. GB/T 14892-2006. Noise limit and measurement method of urban rail transit train. Beijing: China Standard Publishing House, 2005.(in Chinese).
[20] P J Remington. Wheel/rail rolling noise, I: Theoretical analysis. *Journal of the Acoustical Society of America*, 1987, 81: 1805-1823.
[21] T W Wu. Boundary element acoustics. *Wit Press Southampton*, 2000.
[22] E Verheijen, B A Van. Definition of track influence: roughness in rolling noise. *Harmonoise deliverable D12 part 1*, appendix 7 HAR12TR-020813-AEA10, 2003.
[23] R A Clark, P Foster. On the mechanics of rail corrugation formation. *Vehicle System Dynamics*, 1983, 12: 35-39.
[24] X Zhou, J Han, Y Zhao, et al. Characteristics of vibration and sound radiation of metro resilient wheel. *Chinese Journal of Mechanical Engineering*, 2019, 32: 67.
[25] G Xie , P D Allen , S D Iwnicki. Introduction of falling friction coefficients into curving calculations for studying curve squeal noise. *Vehicle System Dynamics*, 2006, 44(Suppl. 1): 261-271.